AD-A143 241 PROPERTIES OF UV-CURABLE POLYURETHANE ACRYLATES: EFFECT 1/1
OF REACTIVE DILUENT(U) WISCONSIN UNIV-MADISON DEPT OF
CHEMICAL ENGINEERING T A SPECKHARD ET AL. 20 JUN 84
UNCLASSIFIED N00014-83-K-0423 F/G 11/9 NL

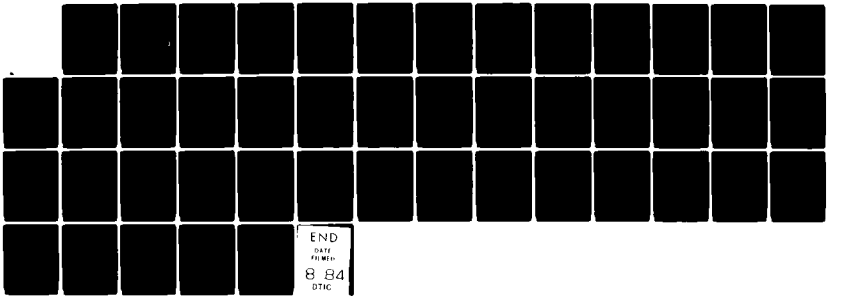

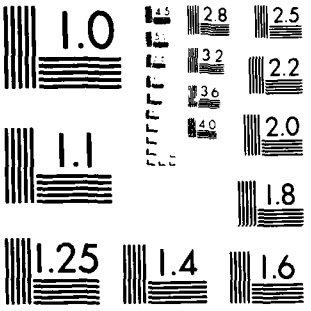

SECURITY CLASSIFICATION OF THIS PAGE (When Data Entered)

(12)

| REPORT DOCUMENTATION PAGE | | READ INSTRUCTIONS BEFORE COMPLETING FORM |
|---|---|---|
| 1. REPORT NUMBER: 4 | 2. GOVT ACCESSION NO. | 3. RECIPIENT'S CATALOG NUMBER |
| 4. TITLE (and Subtitle): Properties of UV Curable Polyurethane Acrylates: Effect of Reactive Diluent | | 5. TYPE OF REPORT & PERIOD COVERED: Interim Technical Report<br>6. PERFORMING ORG. REPORT NUMBER |
| 7. AUTHOR(s): T.A. Speckhard, K.K.S. Hwang, S.B. Lin, S.Y. Tsay, M. Koshiba, Y.S. Ding, and S.L. Cooper | | 8. CONTRACT OR GRANT NUMBER(s): N00014-83-K-0423 |
| 9. PERFORMING ORGANIZATION NAME AND ADDRESS: University of Wisconsin, Department of Chemical Engineering, Madison, WI 53706 | | 10. PROGRAM ELEMENT, PROJECT, TASK AREA & WORK UNIT NUMBERS |
| 11. CONTROLLING OFFICE NAME AND ADDRESS: Office of Naval Research, Code 413, Arlington, VA 22217 | | 12. REPORT DATE: June 20, 1984<br>13. NUMBER OF PAGES |
| 14. MONITORING AGENCY NAME & ADDRESS (if different from Controlling Office) | | 15. SECURITY CLASS. (of this report): Unclassified<br>15a. DECLASSIFICATION/DOWNGRADING SCHEDULE |
| 16. DISTRIBUTION STATEMENT (of this Report): Distribution unlimited | DISTRIBUTION STATEMENT A<br>Approved for public release<br>Distribution Unlimited | |
| 17. DISTRIBUTION STATEMENT (of the abstract entered in Block 20, if different from Report) | DTIC ELECTE JUL 19 1984 S B | |
| 18. SUPPLEMENTARY NOTES: To be published in Journal of Applied Polymer Science | | |
| 19. KEY WORDS (Continue on reverse side if necessary and identify by block number): Polyurethane, Acrylate, UV Curable, Reactive Diluent | | |
| 20. ABSTRACT (Continue on reverse side if necessary and identify by block number): See Accompanying abstract | | |

DD FORM 1 JAN 73 1473 EDITION OF 1 NOV 65 IS OBSOLETE

S N 0102-LF-014-6601

SECURITY CLASSIFICATION OF THIS PAGE (When Data Entered)

ABSTRACT

Several families of UV-cured polyurethane acrylates were synthesized and the effects of reactive diluent type and content on their physical properties were investigated. Increasing reactive diluent content promoted the development of a second, high glass transition temperature phase in all the materials, thereby leading to increased strength and modulus. Changes in the extensibility of the samples upon addition of reactive diluent were inversely related to the effect of the diluent on the crosslink density. The effects of using different reactive diluents (di-, tri- and tetraethylene glycol diacrylate and N-vinyl pyrrolidone) on the physical properties of the samples were attributed to differences in the softening point ($T_g$) of the homopolymer reactive diluents and the relative compatibility of the reactive diluents with the urethane acrylate segments.

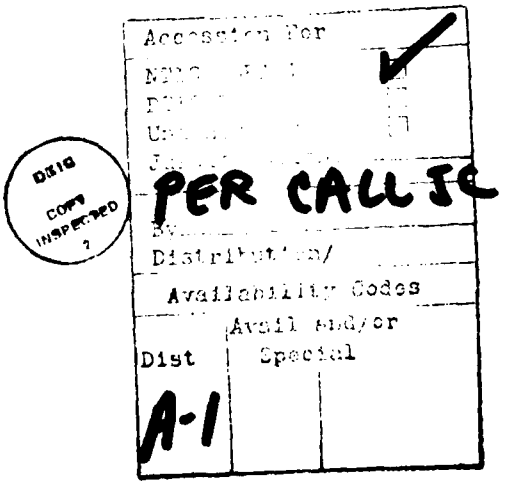

# Properties of UV Curable Polyurethane Acrylates: Effect of Reactive Diluent

T.A. Speckhard, K.K.S. Hwang[a], S.B. Lin[b],
S.Y. Tsay[c], M. Koshiba[d], Y.S. Ding, and S.L. Cooper

Department of Chemical Engineering
University of Wisconsin
Madison, WI 53706

April 1984

Revised

June, 1984

[a] Current address: Life Science Sector, 3M Center, St. Paul, Minnesota

[b] Current address: R&D Syntex Ophthalmics, Inc., Phoenix, AZ

[c] Current address: Chemical Engineering, National Cheng Kung University
Tainan, Taiwan, R.O.C.

[d] Current address: Japan Synthetic Rubber Co., Kawasaki, Japan

Code UWChE: DJP 58-TAS

## I. INTRODUCTION

High intensity radiation from electron beams or ultraviolet sources has been shown to be an effective means to initiate polymerization in reactive oligomer systems (1-5). The advantages of this technology include higher throughput, savings in energy, and reduced or eliminated solvent emissions compared to solvent-based systems, since most formulations are 100% reactive oligomeric liquids (2). The major components of radiation curable systems are the reactive oligomer, reactive diluent, and photoinitiator. Other components which often appear in these systems include non-reactive modifiers, pigments, flow control additives, and plasticizers.

Among commercially important candidates, acrylated urethanes are most often employed as oligomers because these materials combine the high abrasion resistance, toughness, high tear strength, and good low temperature properties of polyurethanes (6,7) with the superior optical properties and weatherability of polyacrylates. In general, a reactive mixture of urethane oligomer tipped with acrylic functionality is combined with vinyl monomers (reactive diluents) which are added to make harder products and/or to reduce the viscosity of the precursor liquid to obtain better processibility. Commercial urethane acrylate oligomers are normally prepared by a two-step procedure. Typically, polyether or polyester macroglycols are sequentially tipped by an aromatic diisocyanate such as toluene diisocyanate (TDI), xylidine diisocyanate (XDI) or isophorone diisocyanate (IPDI), and then by 2-hydroxyethylacrylate (HEA) or 2-hydroxyethylmethacrylate (HEMA) (8-10). It is also possible to react the diisocyanate first with a deficiency of HEA or HEMA and then combine that adduct with the polyol. With and without combination of acrylate monomers, these systems are highly responsive to radiation, producing strong crosslinked films.

UV irradiation induced polymerization is accomplished by incorporation

of suitable ketone type initiators usually in combination with accelerators or proton donors (11,12) which produce free radicals upon exposure to light of appropriate wavelength. This technology is now extensively used in the printing industry, where photoreproduction is possible, and in coating applications (7). Only recently, however, have any publications appeared describing the physical properties of urethane acrylates in any detail (2,13-21).

In previous reports from this laboratory (13,14), structure-property studies have concentrated on the effects of reactive oligomer type and molecular weight since the reactive oligomer is generally considered to be the most important component in determining the mechanical properties of the material (2). Considerably less attention in the literature has been directed at understanding the effects of the reactive diluent type and content on the physical properties of UV-curable urethane acrylates. Schmidle (2) investigated the effects of several different reactive diluents on the properties of Uvithane® materials. He noted a one hundred-fold decrease in the viscosity of the material (prior to curing) upon addition of 30-40% mono- or difunctional reactive diluent. The addition of 50-60% of a trifunctional reactive diluent (trimethylolpropane triacrylate - TMPTA) was necessary to achieve an equivalent decrease in viscosity. Generally, the addition of a monofunctional acrylate reactive diluent such as benzyl acrylate led to a decrease in modulus and an increase in elongation at break with tensile strength staying approximately constant. The addition of 1,6 hexanediol diacrylate, TMPTA, or N-vinylpyrrolidone (NVP), however, led to an increase in modulus and lower elongation. Oraby and Walsh (15,16) in an extensive study of the properties of electron beam-cured urethane acrylates noted the effects of incorporating 25 weight percent of several

different reactive diluents. They found the response of the reactive diluent/oligomer systems to electron beam radiation to be comparable to that of the pure oligomer system with some reactive diluents leading to a slightly higher response and others to a slightly lower response. In general, reactive diluents with a higher degree of unsaturation (i.e. difunctional compared with monofunctional) were found to have a higher response to radiation. One exception was NVP which has only one vinyl group, yet was found to lead to a higher response rate to radiation. Addition of any of the reactive diluents led to the expected dramatic decrease in viscosity relative to the pure oligomer system.

The effects of adding reactive diluents on the tensile properties were interpreted by Oraby and Walsh (15) in light of a proposed structure for urethane acrylate materials. Oraby and Walsh postulated that these materials should possess a multirayed, star-shaped crosslink structure where the average crosslink functionality would equal the average degree of polymerization of the double bonds. They suggested that a high degree of crosslinking was responsible for the poor extensibility (< 200%) of these materials. The authors hoped that copolymerizing the oligomer with a reactive diluent would serve to break up the star-shaped crosslinking and thereby increase the flexibility and elongation of the material. Unfortunately, except for N,N'-diethylaminoethyl acrylate (DEAEA), addition of the reactive diluents led to a decrease or no change in elongation at break, while in most cases the modulus was increased. The addition of DEAEA, however, was found to greatly increase the extensibility (> 400%) of the films while the breaking strength remained practically constant. This behavior was attributed to DEAEA having a significant chain transfer constant which would reduce the degree of polymerization of the acrylic

end groups thereby reducing the crosslink density.

Koshiba et al. (13) studied the effects of varying reactive diluent content (0, 10, or 25% NVP) on the properties of urethane acrylates based on polytetramethylene oxide (PTMO), HEA, and either TDI or IPDI. For all the materials studied increasing NVP content was found to greatly increase strength, toughness, and modulus. For one phase materials (based on 650 molecular weight PTMO) increasing NVP content was reflected in an increased glass transition temperature, a slightly increased degree of crosslinking and reduced extensibility. At 25 wt.% NVP, the sample's $T_g$ was greater than room temperature resulting in brittle behavior under stress. For two phase materials (based on 2000 molecular weight PTMO), increasing NVP content resulted in an increase in the amount and glass transition temperature of the urethane acrylate (hard segment) phase while the $T_g$ of the polyether (soft segment) phase was unaffected. Increasing NVP content did not affect the crosslink density yet elongation at break did improve slightly.

Koshiba et al. (13) also studied a few samples based on polyethyleneglycol diacrylate (PEGDA) as a reactive diluent. All of the PEGDA samples studied were two phase materials and addition of PEGDA increased the amount of the hard segment/reactive diluent phase. However, the $T_g$ of the hard segment phase did not increase upon addition of PEGDA. This result was attributed to the lower $T_g$ of PEGDA compared to NVP and was cited as the reason why the toughness of the material was not improved by adding PEGDA. (Addition of PEGDA led to slightly greater strength but lower elongation.)

In this investigation, the results of a systematic study on the effects of reactive diluent type and concentration are described. The materials

studied were based on four different reactive diluents: PEGDA (P), NVP (N), diethyleneglycol diacrylate (DEGDA) or (D), and triethyleneglycol diacrylate (TEGDA) or (T) -- see Figure 1. Reactive oligomers used included materials based on TDI, HEMA, and PTMO (similar to materials studied by Koshiba et al. (13), except HEMA is used instead of HEA). Two families of materials based on isocyanatoethyl methacrylate (IEM) were also investigated. IEM combines the acrylate and urethane functionalities into one molecule thereby eliminating one step in the oligomer synthesis (14,22). Either functional group can react independently, usually without affecting the latent reactivity of the other group (22). The effects of polyol type and molecular weight on the properties of IEM based urethane acrylates have been described (14). In this study, two families of IEM materials based on either polycarbonate (CB) or PTMO (ET) polyols were studied. All of the materials studied are listed in Table 1. Sample designation codes indicate whether the sample is IEM or TDI-HEMA (T) based, the polyol type (CB or ET) and molecular weight, and the weight percent and type (N, D, T or P) of reactive diluent. For example, IEM-CB1020-25T indicates a 1020 molecular weight polycarbonate, IEM based material with 25 weight percent TEGDA. The effects of reactive diluent type and content on the properties of UV-cured urethane acrylates were investigated using differential scanning calorimetry, dynamic mechanical spectroscopy, and tensile testing.

## II. EXPERIMENTAL

### A. Materials and Synthesis

Isocyanatoethyl methacrylate (IEM) was kindly provided by M.R. Thomas of Dow Chemical and had a purity greater than 99% with 150 ppm of 2,6-di-t-butyl 4-methylphenol (ionol) inhibitor (22). It was used as received.

Polycarbonate polyols (CB) (Vulkollan 2020) were received through the courtesy of Dr. H. Hespe of Bayer. Hydroxyethyl methacrylate (HEMA) was acquired from Aldrich Chemical Co. Polytetramethylene oxide (ET) was obtained from Quaker Oats Chemical Co. These materials were used after vacuum dehydration for at least one day. Toluene diisocyanate (20/80 mixture of 2,6 and 2,4 isomers) (TDI) was used as received from BASF Wyandotte. The procedure used to synthesize these materials has been described in detail (14).

IEM based UV-curable urethane acrylate oligomers were synthesized by slowly adding one mole of dehydrated polyol into a nitrogen-purged reaction flask containing two moles of IEM. The temperature was kept below 45°C to avoid thermal polymerization of the vinyl groups. About .15 wt.% stannous octoate (M and T Chemicals) was added and two hours were allowed to complete the reaction. 100 ppm of hydroquinone was added as an inhibitor to ensure stable shelf life before UV-curing. TDI based urethane acrylates were synthesized by adding an equimolar amount of dehydrated HEMA dropwise to TDI under a nitrogen atmosphere. Again, the temperature was kept below 45°C to avoid thermal polymerization of the vinyl groups. When the TDI/HEMA reaction mixture temperature started to drop, a stoichiometric quantity of dehydrated polyol was added along with stannous octoate catalyst. The mixture was agitated for two hours and heated to 70°C to complete the reaction.

The photoinitiator used was a one-to-one mixture of 2,2'-diethoxyacetophenone (Polysciences) and N-methyldiethanolamine (Aldrich). Approximately .6 wt% of the initiator mixture was added to the urethane acrylate oligomer prior to curing. The reactive diluents used in this study were N-vinylpyrrolidone (NVP) (Aldrich), diethyleneglycol diacrylate (DEGDA), triethyleneglycol diacrylate (TEGDA), and polyethyleneglycol diacrylate

(PEGDA). The diacrylate materials were received from Sartomer Chemical Co.; the chemical structures of the reactive diluents are shown in Figure 1.

B. Sample Preparation

The mixture of urethane acrylate oligomer, 0.6 wt% photoinitiator and reactive diluent was heated slightly above ambient temperature to ensure homogeneous mixing. The liquid prepolymers were poured into teflon coated molds of varied thickness. Samples were about 0.2-0.3 mm in thickness for tensile specimens and 50 μm for dynamic mechanical analysis. To perform kinetic studies prepolymers were also cast directly on KBr plates with a thickness that allowed at least 30% transmission in the infrared region (1000-4000 $cm^{-1}$) before and after UV-curing.

The samples were irradiated from one side under a nitrogen atmosphere using a bank of 20W mercury lamps ($\lambda$ = 365 nm) as the irradiation source. An irradiation time of 10 minutes was found to cure specimens satisfactorily and was used for all of the samples.

C. Characterization Methods

1. Viscometry

The viscosity of selected prepolymers was characterized using a Brookfield viscometer. Some polycarbonate based prepolymers were solid at ambient temperature; therefore, for comparison purposes, all viscosity measurements were performed at 40°C. As expected, the addition of reactive diluent resulted in a large decrease in bulk viscosity. Viscosity data on some of these materials have been presented previously (14).

2. Soxhlet Extraction

The gel fraction of the cured samples was determined by Soxhlet extraction using toluene for 24 hours. The insoluble gel fraction was dried under vacuum for about two days and weighed to determine the gel fraction.

(PEGDA). The diacrylate materials were received from Sartomer Chemical Co.; the chemical structures of the reactive diluents are shown in Figure 1.

B. Sample Preparation

The mixture of urethane acrylate oligomer, 0.6 wt% photoinitiator and reactive diluent was heated slightly above ambient temperature to ensure homogeneous mixing. The liquid prepolymers were poured into teflon coated molds of varied thickness. Samples were about 0.2-0.3 mm in thickness for tensile specimens and 50 μm for dynamic mechanical analysis. To perform kinetic studies prepolymers were also cast directly on KBr plates with a thickness that allowed at least 30% transmission in the infrared region (1000-4000 $cm^{-1}$) before and after UV-curing.

The samples were irradiated from one side under a nitrogen atmosphere using a bank of 20W mercury lamps ($\lambda$ = 365 nm) as the irradiation source. An irradiation time of 10 minutes was found to cure specimens satisfactorily and was used for all of the samples.

C. Characterization Methods

1. Viscometry

The viscosity of selected prepolymers was characterized using a Brookfield viscometer. Some polycarbonate based prepolymers were solid at ambient temperature; therefore, for comparison purposes, all viscosity measurements were performed at 40°C. As expected, the addition of reactive diluent resulted in a large decrease in bulk viscosity. Viscosity data on some of these materials have been presented previously (14).

2. Soxhlet Extraction

The gel fraction of the cured samples was determined by Soxhlet extraction using toluene for 24 hours. The insoluble gel fraction was dried under vacuum for about two days and weighed to determine the gel fraction.

3. Infrared Spectroscopic Measurements

Infrared spectra of thin polymer films cast on KBr plates were taken before and after UV irradiation using a Nicolet 7199 Fourier-transform infrared spectrometer. The characteristic C=C absorption of urethane acrylate at 1635 $cm^{-1}$ was used to determine the extent of photoinitiated vinyl polymerization. The N=C=O stretching near 2270 $cm^{-1}$ was used to monitor the extent of reaction in prepolymer preparations.

4. Stress-Strain Measurements

Uniaxial stress-strain measurements at room temperature were made using a table model Instron tensile testing machine with a crosshead speed of 0.5 inch/min. Dumbbell shaped film samples with a gauge length of 1.5 inch were stamped out with an ASTM 412 die. The engineering stress was calculated as the ratio of force to initial cross-sectional area. Reported data were the average of three tests.

5. Dynamic Mechanical Measurements

Dynamic mechanical data were collected at 110 Hz using a Toyo Rheovibron DDV-IIC apparatus which was controlled automatically by a LSI-11/03 microprocessor. Film samples of about 20 x 2 x 0.05 mm were tested under a nitrogen blanket from -150°C to 200°C at a heating rate of 2°C/min.

6. Differential Scanning Calorimetry

DSC thermograms of urethane acrylate prepolymers as well as the UV-cured polymers were recorded using a Perkin-Elmer DSC-II equipped with a thermal analysis data station. The experiments were carried out from -120°C to 180°C at a heating rate of 20°C/min under a helium purge. The DSC thermograms were normalized to equivalent sample weight to facilitate comparisons.

## III. RESULTS AND DISCUSSION

### A. The Extent of Photopolymerization

The UV-initiated polymerization process was monitored by infrared spectroscopy and the results were described previously (14). IR spectra were taken prior to and after one minute of UV irradiation. The twice expanded difference (after - before) spectrum was plotted to show spectroscopic changes resulting from the curing process. The complete disappearance of the C=C band at 1635 $cm^{-1}$ indicated that the vinyl polymerization reaction had occurred. Beachell et al. (23,24) reported on the gradual UV-induced decomposition of urethane compounds. In the present case, minimal changes in the spectral regions where urethane decomposition products absorb indicate urethane stability during the photopolymerization. Thus the primary photochemical reaction is polymerization of the vinyl groups. The extent of photopolymerization was also measured by Soxhlet extraction to determine the gel fraction. Generally, samples were found to contain greater than .95 gel fraction although lower values were occasionally found presumably due to inhibition of the polymerization by dissolved oxygen. Only samples with a gel fraction greater than .95 were used in the structure-property studies.

### B. Thermal Properties

Figure 1 shows the chemical structure of the various reactive diluents used in this study and lists their glass transition temperature as measured by DSC. The three diacrylate materials were chosen to provide a systematic change in chemical structure as well as glass transition temperature. The D and T materials also provide glass transition temperatures between the P and N materials studied previously (13). It should be noted that the absolute value of the glass transition temperature of these materials may be

influenced to a large extent by absorption of moisture (21,25). For example, a glass transition temperature of 73°C for poly-NVP indicates a moisture content of approximately 10% (25). (Dry poly-N$^{VP}$ has been reported to have a $T_g$ of 175°C (25).) However, in this study only the relative trend of reactive diluent glass transition temperatures is of primary importance. Also, the effect of moisture in the urethane acrylate/reactive diluent materials should be less than its effect in the pure reactive diluent samples. Olson and Webb (21) have investigated the effect of humidity on the glass transition temperature of urethane acrylates in greater detail.

DSC thermograms for several families of urethane acrylates are shown in Figures 2-4. Glass transition temperatures determined by DSC are listed in Table 1. Figure 2 displays thermograms for the T-ET2000 series materials. All of the materials in Figure 2 exhibit a single glass transition at approximately -73°C. The lack of other thermal events might be indicative of a one phase material; however, it has been previously found that thermograms of similar materials demonstrating a two phase morphology (by dynamic mechanical analysis) often do not exhibit a melting endotherm or glass transition associated with the urethane acrylate (hard segment) phase (13,14). In fact, in this case the constancy of the glass transition temperature is indicative of a two phase material. In one phase materials, increasing the amount of reactive diluent will generally raise the glass transition temperature of the material (13,14). Therefore, the behavior exhibited in Figure 2 is attributed to a two phase morphology where the reactive diluent is associated with the hard segment phase; thus the glass transition temperature of the polyol or soft segment is unaffected by reactive diluent type or content.

Figure 3 shows DSC thermograms for the IEM-ET1000 series materials.

Previous work would indicate that these materials have a low degree of phase separation (13,14). For all of the materials shown in Figure 3 the glass transition is much broader and less distinct than the transitions observed for the well phase separated T-ET2000 materials (Figure 2). It should also be noted that again there are no distinct high temperature transitions that would be associated with the development of a hard segment phase. Looking first at the NVP based materials, a constant glass transition temperature which is slightly higher than that of the control (0% reactive diluent) material is noted. This behavior can be attributed to the interaction of two different effects. The slight rise in the $T_g$ indicates some interaction between NVP and the soft segment phase. The fact that the $T_g$ does not continue to increase with increasing NVP content indicates that most of the NVP is associated with a second (hard segment) phase. An alternate explanation based only on the DSC data could attribute the slight rise in $T_g$ to an increase in the crosslinking density (thereby increasing the restrictions on the polyol chains) upon addition of NVP. However, this explanation is not supported by previous work (13,14) or the dynamic mechanical data presented in the next section. The materials incorporating TEGDA (T) as a reactive diluent also demonstrate behavior that can be attributed to competing effects. In this case adding 10% TEGDA results in a noticeable decrease in the glass transition temperature which is ascribed to improved phase separation. Further addition of TEGDA (to 25%) does result in an increase in $T_g$ that may be due to an increase in the crosslink density or an increased interaction between TEGDA and the soft segment phase.

DSC thermograms for the IEM-CB1020 series materials are shown in Figure 4. Again, these materials would be expected to exhibit a low

degree of phase separation. The thermograms which exhibit one broad glass transition and no high temperature thermal events are similar to those of the IEM-ET1000 series materials. Addition of the various reactive diluents causes a slight decrease in the glass transition temperature that can be attributed to improved phase separation. It appears that TEGDA and NVP are slightly more efficient in promoting phase separation than PEGDA.

C. Mechanical Properties

Dynamic mechanical storage modulus and loss factor curves are shown for several families of urethane acrylates in Figures 5, 6, 8 and 10. Stress-strain curves for the same families are shown in Figures 7, 9, and 11 while tensile properties (Young's modulus, stress at break, and elongation at break) are listed in Table 1. Figure 5 shows the dynamic mechanical data for the T-ET2000 series materials with 10% reactive diluent content (P, T, or D). The sample with 0% reactive diluent content (T-ET2000-0) is included for comparison. The dynamic storage modulus data indicate that incorporation of any of the reactive diluents results in increased modulus from -50 to 50°C. The PEGDA and TEGDA based materials also seem to have a higher crosslink density as indicated by the level of the high temperature (> 100°C) modulus.

The loss factor curves (Figure 5) exhibit three distinct peaks. The low temperature (~-120°C) peak is associated with localized motion of the methylene sequences of the polyether segments (6) while the overlapping peaks, centered at approximately -50 and 60°C, are indicative of a two phase microstructure and can be attributed to glass transitions of the polyether and urethane acrylate/reactive diluent phases, respectively. The reactive diluent is assumed to associate primarily with the urethane acrylate phase since the addition of reactive diluent lowers the loss factor peak associated

with the polyether segments (indicating a lower weight percent of that phase) and increases the height of the urethane acrylate loss factor peak. Also, as noted above in the DSC data, the soft segment glass transition temperature in these materials is unaffected by the addition of reactive diluent. This behavior can be partially ascribed to the fact that the highly polar reactive diluents are more compatible with the more polar urethane acrylate segments compared with the less polar polyol segments. Thus, any reactive diluent homopolymer produced during the curing process will tend to associate with the urethane acrylate phase. Egboh (26) studied blends of poly-NVP and segmented polyurethanes and found that the poly-NVP and urethane hard segments were compatible. He attributed the compatibility to similar polarities and hydrogen bonding between the urethane hydrogen and the NVP carbonyl. Since diacrylates have two carbonyl groups per molecule they may be even more compatible with urethane hard segments than NVP. Another factor to be considered is that reactive diluent units that copolymerize with urethane acrylate groups will tend to be included in the urethane acrylate phase.

Figure 5 also shows that differences between materials based on the various reactive diluents are small, at least at this reactive diluent content (10%). At room temperature the modulus increases in the order P<T<D which also parallels the trend of increasing glass transition temperature (Figure 1).

The dynamic mechanical data for the T-ET2000-25 series materials are exhibited in Figure 6. The data for sample T-ET2000-0 are again included for comparison. Comparing the data of Figures 5 and 6 shows that increasing the reactive diluent content to 25% accentuates the trends noted for the 10% reactive diluent materials. The dynamic modulus in the range of -50 to

50°C is increased dramatically upon addition of 25 wt.% of the reactive diluent. The dynamic storage modulus at room temperature appears to increase with reactive diluent type in the order P<T<D. The trend of modulus with reactive diluent type could be attributed to increased compatibility of the reactive diluent with the urethane acrylate phase leading to a greater proportion of the hard segment phase and a greater likelihood of copolymerization of the reactive diluent and the acrylate groups. Thus, since on the basis of chemical structure DEGDA should be most compatible with the urethane acrylate segments (DEGDA has the least amount of aliphatic component) and PEGDA the least compatible, the observed trends of modulus with reactive diluent type is reasonable. Figures 5 and 6 show that the effect of adding and increasing the amount of any of the reactive diluents increases the crosslink density as measured by the level of the storage modulus at high temperatures (>100°C). In this case, the concept of Oraby and Walsh (15) whereby copolymerization with a reactive diluent serves to reduce the crosslink density relative to the pure oligomer is not valid. This concept appears to only be applicable to monofunctional reactive diluents since even Oraby and Walsh (15) expected the addition of a trifunctional reactive diluent to increase the crosslink density. In general (2), the addition of monofunctional reactive diluents decreases crosslink density while the addition of multifunctional reactive diluents results in increased crosslink density. The trend of increased crosslink density with reactive diluent type in Figure 6 is D>T>P which could be reflective of the chain length between the acrylate functionalities in the reactive diluent. That is, the shorter chain length between the acrylate groups in DEGDA relative to PEGDA could result in a more highly crosslinked structure for the DEGDA based material. However, the differences in chain

length are fairly small and the trend of crosslink density with reactive diluent type may be more attributable to differences in compatibility of the reactive diluents with the oligomer and/or the effectiveness of the reactive diluents to act as chain transfer agents. Finally, the trend of hard segment compatibility with reactive diluent type can be readily observed from the loss factor data shown in Figure 6. The height of the peak associated with the soft segment glass transition becomes lower as the reactive diluent becomes less compatible with the polyether segments. The reverse trend with the hard segment glass transition loss peak is not as distinct, probably because of differences in the breadth and position of the peak. (Note that the hard segment $T_g$ does increase with reactive diluent type in the same order as the $T_g$ of the reactive diluent homopolymers.)

Stress-strain curves for the T-ET2000 series materials are shown in Figure 7. Data for some materials based on 650 molecular weight PTMO are also included; these materials would be expected to possess a one phase morphology (13). For the T-ET2000 series materials the data in Figure 7 demonstrate that increasing reactive diluent content increases the tensile strength and modulus while slightly decreasing the elongation at break. It should be noted that the elongation at break for all of these materials is rather low. Oraby and Walsh would attribute this behavior to a high degree of crosslinking due to a high average degree of polymerization of the urethane acrylate groups. However, the differences in crosslink density determined from the dynamic mechanical data for the T-ET2000-25 series materials are not accompanied by changes in the elongation at break (Figure 7). In fact Figure 7 shows that there is no difference in elongation at break with reactive diluent type for any of the families of materials. The modulus and stress at break do change with reactive diluent type in the

order D>T>P for all of the families of materials shown in Figure 7. This trend parallels the trend of room temperature modulus for the T-ET2000 series materials noted in Figures 5 and 6. Again this behavior would be expected based on the differences in glass transition temperature and chemical structure of the reactive diluent. It is interesting to note that the effect of increasing the reactive diluent content from 10 to 25% outweighs the effect of changing reactive diluent type.

Table 1 lists tensile properties for the materials shown in Figure 7 and also includes data for an NVP based sample, T-ET2000-25N, investigated previously (14). A comparison of sample T-ET2000-25N with the other T-ET2000-25 series materials shows that the NVP based material has superior tensile strength, modulus, and elongation. The increase in properties with NVP compared to the diacrylate materials is probably due to the higher glass transition of poly-NVP and possibly a greater compatibility with the urethane acrylate segments leading to a higher degree of phase separation.

Figure 8 shows dynamic mechanical storage modulus and loss factor curves for the IEM-ET1000 materials with varying NVP content. The dynamic storage modulus data show an increase in modulus in the region from -50 to 50°C as the weight percent of NVP increases; there is a particularly large increase between 10 and 25 wt.% NVP. It is interesting to note that, in this case, increasing reactive diluent content does result in a lower crosslink density as measured by the level of the storage modulus at high temperatures. This as noted above is probably due to the monofunctional nature of NVP. The opposite trend was observed for PEGDA, TEGDA, and DEGDA in the T-ET2000 series materials and may partially explain the better extensibility of the NVP based sample of that family. NVP could also be a more effective chain transfer agent than the diacrylate reactive diluents. It should also be

noted that the T-ET2000 materials were already well phase separated prior to adding reactive diluent, whereas the degree of phase separation for the IEM based samples increases markedly with reactive diluent content. Thus, it may be that the improvement in phase separation is leading to greater extensibility in the IEM samples. (Note the higher elongation at break of T-ET2000-0 compared with IEM-ET1000-0 (Table 1).)

The large increase in modulus between the 10 and 25 wt.% NVP samples can be understood on the basis of the loss factor data in Figure 8. Samples IEM-ET1000-0 and IEM-ET1000-10N exhibit one broad glass transition peak indicative of a one phase or poorly phase separated material. On the other hand, samples IEM-ET1000-25N and IEM-ET1000-40N exhibit two overlapping peaks attributable to separate soft and hard segment phases. Thus, increasing NVP content from 10 to 25 wt.% dramatically improves the degree of phase separation leading to a large increase in modulus.

Stress-strain curves for the IEM-ET1000 series materials are shown in Figure 9. Increasing NVP content leads to greater strength, modulus, and elongation at break. These trends are in agreement with the dynamic mechanical data discussed above that exhibited greater modulus and lower crosslink density with increasing NVP content. Table 1 lists the tensile properties of the materials shown in Figure 9 along with two samples based on TEGDA for comparison. In contrast with the T-ET2000 series materials where the NVP based samples exhibited greatly improved properties relative to samples based on the diacrylate reactive diluents, in this case the NVP based samples have slightly better elongation but lower stress at break compared to the materials based on TEGDA with equivalent reactive diluent contents. The lower strength of the NVP based materials may be due to a lower degree of phase separation as indicated by the higher soft segment

$T_g$ measured by DSC.

Figure 10 displays dynamic mechanical data for the IEM-CB1020 series materials. For this family of materials the modulus in the region from -50 to 50°C increases with reactive diluent type in the order P<N<T with the PEGDA material showing only slight improvement compared to the control while the moduli for the NVP and TEGDA samples are similar and greatly increased relative to the control sample. The level of the modulus at high temperatures indicates that adding NVP reduces the crosslink density while adding PEGDA increases the crosslink density (it appears that the addition of TEGDA causes a slight reduction in the crosslink density). As discussed above, this difference is primarily due to the fact that NVP is monofunctional while PEGDA is difunctional although differences in compatibility with the oligomer and chain transfer effects can also influence the trend of crosslink density with reactive diluent type. The loss factor curves for these materials indicate that the control and PEGDA possess a lower degree of phase separation than the TEGDA and NVP based materials (one broad glass transition peak compared with two distinct peaks). This improvement in phase separation is responsible for the large difference in modulus at room temperature. Figure 11 displays stress-strain curves for the IEM-CB1020 series materials. The trend of strength and modulus with reactive diluent type is in agreement with the trend of room temperature dynamic modulus with reactive diluent type (T>N>P). The effect of reactive diluent type on the crosslink density (discussed above) is also reflected in the trend of the elongation at break with reactive diluent type (N>T>control>P).

Comparing the properties of the IEM and TDI-HEMA based materials reveals some interesting trends. As discussed above adding reactive diluent to

the TDI based materials increases the strength and modulus in the order N>D>T>P while for the IEM based samples the order is T>N>P (D not tested). For the IEM based materials addition of reactive diluent generally leads to improved elongation at break while for the TDI based materials this is only true for NVP. This behavior correlates with the fact that adding reactive diluent (D, T, or P) to the TDI based materials leads to a higher crosslink density while adding reactive diluent (T, N, or P) to the IEM based samples leads to a lower crosslink density. Because of the many different factors (compatibility of the reactive diluent with the hard and soft segments, degree of phase separation, effect of reactive diluent as a chain transfer agent, and the extent of copolymerization of the reactive diluent with the urethane acrylate groups) affecting the physical properties of these materials, it is difficult to directly relate the property differences cited above to the differences in chemical structure between TDI-HEMA and IEM and the various reactive diluents. Obviously, more experimental data is needed on such factors as the relative compatibility of the reactive diluent with the hard and soft segments, the efficiency of the various reactive diluents as chain transfer agents, and the extent of copolymerization of the reactive diluents with the urethane acrylate groups, to completely understand the structure-property relationships of these materials. However, it is possible without such data to make some hypotheses concerning the trends cited above.

The trend of increased strength and modulus with reactive diluent type for the T-ET2000 series materials directly parallels the trend of reactive diluent glass transition temperature (N>D>T>P). Since sample T-ET2000-0 is already highly phase separated, the addition of reactive diluent serves primarily to increase the volume fraction of the hard segment phase. Thus, addition of a higher $T_g$ reactive diluent leads to a stronger

material but generally lower elongation. The IEM based control samples, however, exhibit a one phase or poorly phase separated morphology primarily because of their lower polyol molecular weight. Thus, addition of reactive diluent to the IEM based samples seems to improve the degree of phase separation as well as increasing the hard segment content of the IEM based materials. Presumably because of differences in chemical structure leading to differences in compatibility, the diacrylate reactive diluents appear to be more effective at increasing the degree of phase separation in IEM based samples than NVP. (Note the linear aliphatic structure of IEM and the diacrylate materials compared with the cyclic or aromatic natures of TDI and NVP.) Yet, NVP is a higher $T_g$ component whose addition to the hard segment phase will promote increased strength and modulus to a greater extent than the diacrylate materials. These two competing effects result in a trend of increasing strength with reactive diluent type of T>N>P (presumably D>T). The fact that adding reactive diluent (D, T, or P) decreases elongation at break for TDI based samples and increases elongation at break for IEM based samples is partially a result of the greater extensibility and lower crosslink density of the TDI based samples relative to the IEM based materials with 0% reactive diluent content. That is, prior to adding reactive diluent the crosslink density is greater in the IEM based samples leading to lower elongation. Thus, adding reactive diluent to the IEM based samples can lead to a reduction of the crosslink density, probably by copolymerization with the urethane acrylate groups as suggested by Oraby and Walsh (15). For the TDI materials the initially low crosslink density appears to actually increase slightly upon addition of reactive diluent. Possibly, the reduction in viscosity during curing allows for greater polymerization of the urethane acrylate groups. It is also possible

that the effectiveness of the reactive diluents as chain transfer agents is markedly different in the TDI-HEMA and IEM based systems because of the difference in structure or viscosity during the curing process.

## IV. SUMMARY

The effects of reactive diluent type and content on the properties of UV-cured polyurethane acrylate have been investigated using differential scanning calorimetry, dynamic mechanical spectroscopy and tensile testing. For all the materials studied increasing reactive diluent content led to increasing dynamic mechanical and tensile moduli and increasing tensile strength. Addition of reactive diluent to materials with low (< 1100) polyol molecular weights (generally exhibiting a one phase or poorly phase separated morphology) increased the degree of phase separation and the amount of the urethane acrylate/reactive diluent phase. Samples based on a higher polyol molecular weight (2000) exhibited a well defined two phase morphology prior to adding reactive diluent. In this case addition of reactive diluent served primarily to increase the amount of the urethane acrylate/reactive diluent phase. In either case these morphological changes strengthened the material and demonstrated that the reactive diluent was associated primarily with the urethane acrylate segments. This behavior was attributed to greater compatibility between the more polar reactive diluent and urethane acrylate segments compared with the less polar polyol segments and the fact that reactive diluent units that copolymerize with the urethane acrylate groups will tend to be included in the urethane acrylate phase.

For the T-ET2000 series materials the order of increased strength and modulus with reactive diluent type was N>D>T>P. This trend was attributed to the increasing $T_g$ of the reactive diluent since the trend of reactive diluent type with homopolymer reactive diluent $T_g$ is identical. Addition of

the diacrylate reactive diluents led to increased crosslinking and lower elongation; a trend commonly observed in the literature. For the IEM based materials the trend of increased strength and modulus with reactive diluent type was T>N>P. In these samples the greater reinforcing capability of NVP is partially offset by its lower efficiency in promoting phase separation. The IEM based samples with 0% reactive diluent content exhibited low extensibility; addition of any of the reactive diluents decreased the cross-link density and increased elongation.

Acknowledgements:

The authors would like to thank M. R. Thomas of Dow Chemical Co. for supplying the IEM and Dr. H. Hespe of Bayer AG for providing the polycarbonate diols. The authors acknowledge partial support of this research by the Office of Naval Research and the Naval Air Systems Command.

## REFERENCES


1. W. Moreau and N. Viswanathan, ACS Org. Coat. Preprints, 35(1), 108 (1975).
2. C. J. Schmidle, J. Coated Fabrics, 8, 10 (1978).
3. J. V. Crivello, ACS Org. Coat. Preprints, 41, 560 (1979).
4. L. Kushner and R. S. Tu, Modern Plastics, 87 (1983).
5. C. Decker, ACS Polym. Matl. Preprints, 49, 32 (1983).
6. A. Lilaonitkul and S. L. Cooper, "Advances in Urethane Science and Technology", K. C. Frisch and S. L. Reegen, Eds., Technomic Publ. Co., 7, 163 (1979).
7. C. Bluestein, Polym.-Plast. Technol. Eng., 17, 83 (1981).
8. Nippon Kokai Tokkyo Koho, 48-43657 (1973) (Japanese Patent).
9. Nippon Kokai Tokkyo Koho, 46-29525 (1971) (Japanese Patent).
10. U.S. Patent Number 3,907,865 (1975).
11. U.S. Patent Number 2,993,789 (1961).
12. T. Higuchi, in "Photopolymer" edited by T. Tsunoda (CMC, Tokyo, 1977) p. 137.
13. M. Koshiba, K. K. S. Hwang, S. K. Foley, D. J. Yarusso, and S. L. Cooper, J. Materials Sci., 17, 1447 (1982).
14. S. B. Lin, S. Y. Tsay, T. A. Speckhard, K. K. S. Hwang, J. J. Jezerc, and S. L. Cooper, Chem. Engr. Comm., in press.
15. W. Oraby and W. K. Walsh, J. Applied Polym. Sci., 23, 3227 (1979).
16. W. Oraby and W. K. Walsh, J. Applied Polym. Sci., 23, 3243 (1979).
17. L. H. Wadhwa and W. K. Walsh, ACS Org. Coat. Preprints, 42, 509 (1980).
18. K. Park and G. L. Wilkes, ACS Org. Coat. Preprints, 41, 308 (1979).
19. E. G. Joseph, G. L. Wilkes and K. Park, ACS Polymer Preprints, 20, 520 (1979).
20. D. A. Bolon, G. M. Lucas, D. R. Olson, and K. K. Webb, J. Appl. Polym. Sci., 25, 543 (1980).
21. D. R. Olson and K. K. Webb, ACS Org. Coat. Preprints, 39, 518 (1978).
22. M. R. Thomas, ACS Org. Coat. Preprints, 46, 506 (1982).

23. H. C. Beachell, and I. L. Chang, J. Polym. Sci., Part A-1, 10, 503 (1972).

24. H. C. Beachell, and C. P. Ngocson, J. Appl. Polym. Sci., 7, 2217 (1963).

25. Y. Y. Tan and G. Chalua, Polymer, 17, 739 (1976).

26. S. H. Egboh, ACS Polym. Matl. Preprints, 49, 45 (1983).

Table 1

SAMPLE DESIGNATION, TENSILE PROPERTIES AND GLASS TRANSITION TEMPERATURE OF UV-CURED URETHANE ACRYLATES

| SAMPLE DESIGNATION | YOUNG'S MODULUS (MPa) | ELONGATION AT BREAK (%) | STRESS AT BREAK (MPa) | DSC $T_g$ (°C) |
|---|---|---|---|---|
| T-ET650-0 | 29 | 64 | 3.9 | - |
| T-ET650-25T | 34 | 36 | 3.5 | - |
| T-ET650-25D | 57 | 37 | 4.6 | - |
| T-ET2000-0 | 2.0 | 95 | 1.2 | -73 |
| T-ET2000-10P | 3.0 | 80 | 1.3 | -73 |
| T-ET2000-25P | 5.0 | 54 | 1.5 | -74 |
| T-ET2000-10T | 4.0 | 75 | 1.5 | -73 |
| T-ET2000-25T | 9.5 | 52 | 2.0 | -72 |
| T-ET2000-10D | 5.0 | 80 | 1.7 | -73 |
| T-ET2000-25D | 17.0 | 50 | 2.4 | -74 |
| T-ET2000-25N | 80.0 | 136 | 12.0 | -72 |
| IEM-CB1020-0 | 13.9 | 25 | 3.2 | -11 |
| IEM-CB1020-25P | 18.0 | 16 | 2.3 | -13 |
| IEM-CB1020-25T | 45.0 | 37 | 11.2 | -16 |
| IEM-CB1020-25N | 30.0 | 63 | 9.3 | -14 |
| IEM-ET1000-0 | 9.5 | 19 | 1.8 | -59 |
| IEM-ET1000-10N | 9.6 | 25 | 2.2 | -57 |
| IEM-ET1000-25N | 14.1 | 42 | 4.4 | -57 |
| IEM-ET1000-40N | 28.5 | 55 | 5.8 | -57 |
| IEM-ET1000-10T | - | 23 | 2.7 | -69 |
| IEM-ET1000-25T | - | 30 | 6.5 | -64 |

FIGURE CAPTIONS

Figure 1 Monomer structures of reactive diluents, glass transition temperatures of homopolymer reactive diluents and urethane oligomer component structures

Figure 2 DSC thermograms for the T-ET2000 series materials

Figure 3 DSC thermograms for the IEM-ET1000 series materials

Figure 4 DSC thermograms for the IEM-CB1020 series materials

Figure 5 Dynamic mechanical storage modulus and loss factor curves for the T-ET2000-10 series materials

Figure 6 Dynamic mechanical storage modulus and loss factor curves for the T-ET2000-25 series materials

Figure 7 Stress-strain curves for the T-ET2000 and T-ET650 series materials

Figure 8 Dynamic mechanical storage modulus and loss factor curves for the IEM-ET1000 series materials

Figure 9 Stress-strain curves for the IEM-ET1000 series materials

Figure 10 Dynamic mechanical storage modulus and loss factor curves for the IEM-CB1020 series materials

Figure 11 Stress-strain curves for the IEM-CB1020 series materials

URETHANE OLIGOMER COMPONENT STRUCTURES

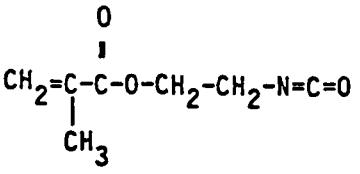

isocyanatoethyl methacrylate (IEM)

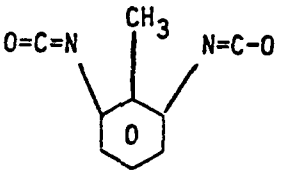

2,6-toluene diisocyanate (T)

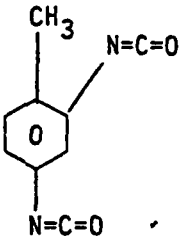

2,4-toluene diisocyanate (T)

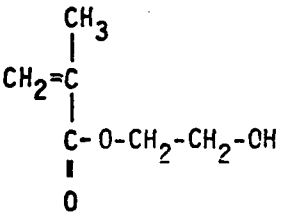

2-hydroxyethyl methacrylate (HEMA)

FIGURE 1

REACTIVE DILUENT STRUCTURES

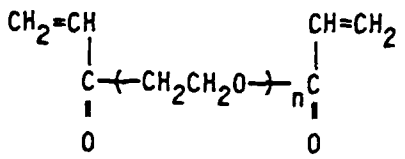

| | | Homopolymer $T_g$°C (DSC) |
|---|---|---|
| n = 2 | diethyleneglycol diacrylate - (D) | 45 |
| n = 3 | triethyleneglycol diacrylate - (T) | 35 |
| n = 4 | tetra(poly)ethyleneglycol diacrylate - (P) | 21 |

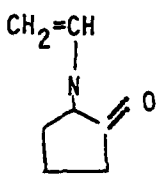

N-vinylpyrrolidone (NVP) - (N) 73

FIGURE 1

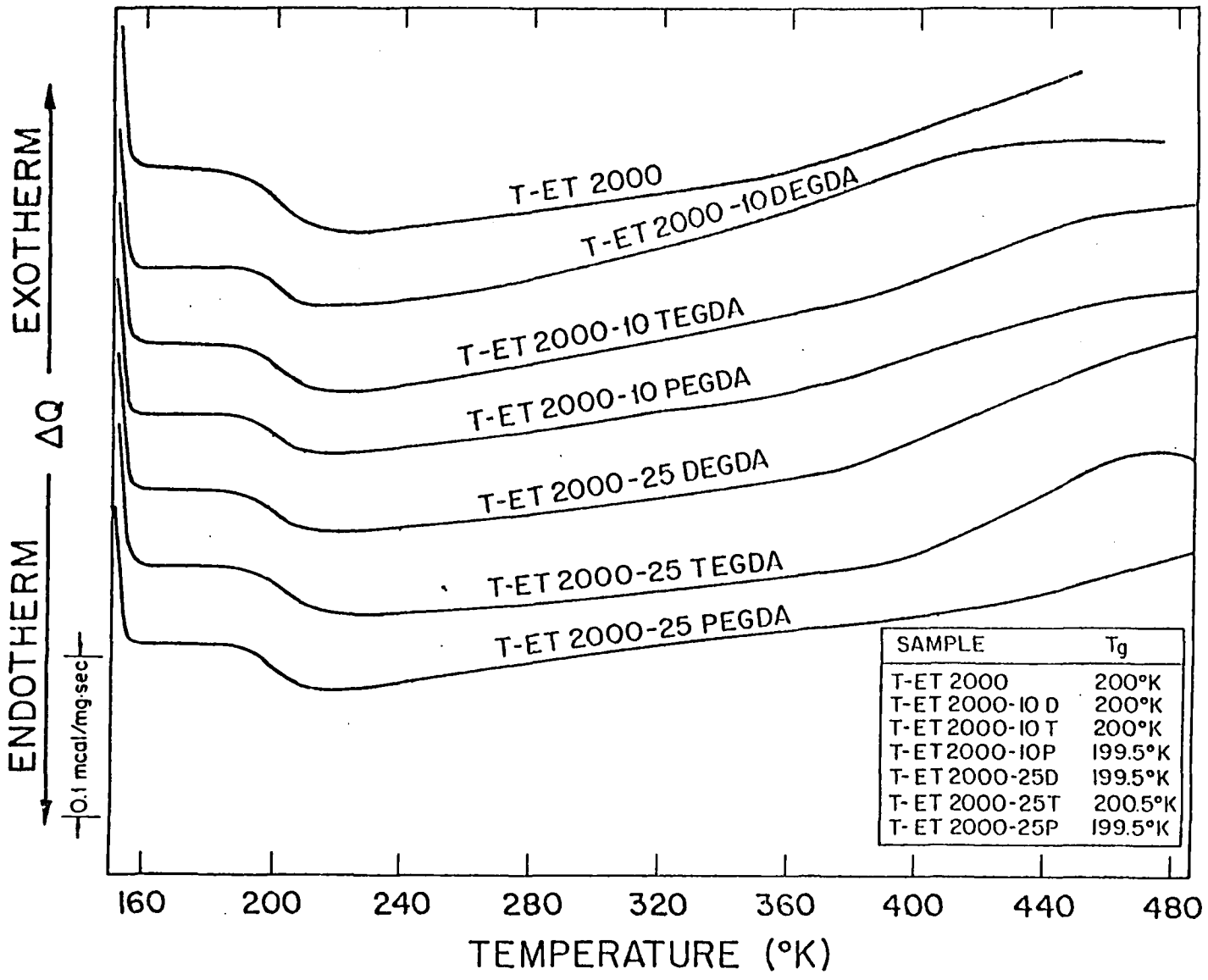
EXOTHERM
ΔQ
ENDOTHERM
0.1 mcal/mg-sec
T-ET 2000
T-ET 2000-10DEGDA
T-ET 2000-10 TEGDA
T-ET 2000-10 PEGDA
T-ET 2000-25 DEGDA
T-ET 2000-25 TEGDA
T-ET 2000-25 PEGDA
SAMPLE | Tg
T-ET 2000 | 200°K
T-ET 2000-10 D | 200°K
T-ET 2000-10 T | 200°K
T-ET 2000-10P | 199.5°K
T-ET 2000-25D | 199.5°K
T-ET 2000-25T | 200.5°K
T-ET 2000-25P | 199.5°K
160
200
240
280
320
360
400
440
480
TEMPERATURE (°K)

FIGURE 2

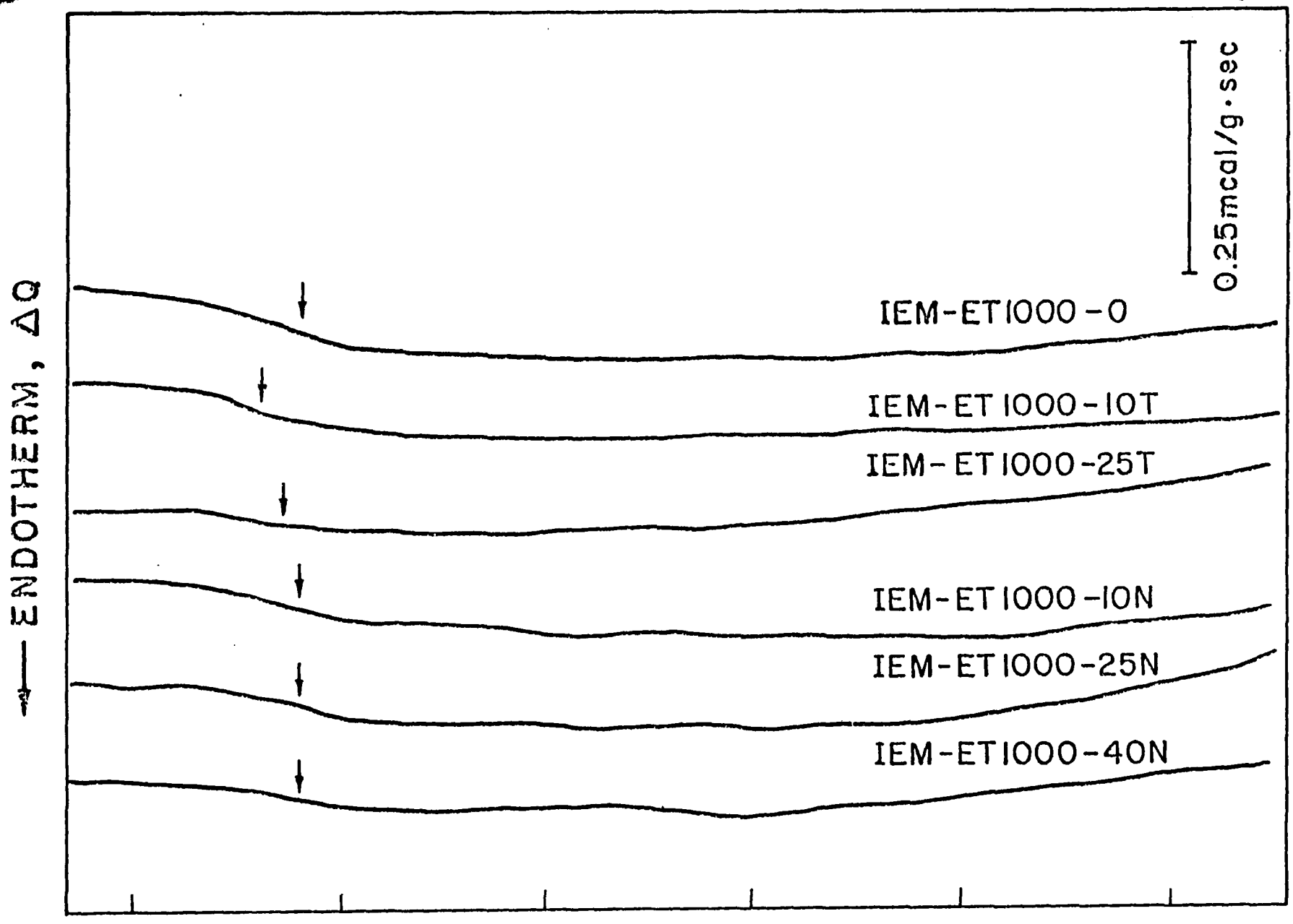
0.25mcal/g·sec
IEM-ET1000-0
IEM-ET1000-10T
IEM-ET1000-25T
IEM-ET1000-10N
IEM-ET1000-25N
IEM-ET1000-40N
ENDOTHERM, ΔQ
-100
-50
0
50
100
150
TEMPERATURE, °C

FIGURE 3

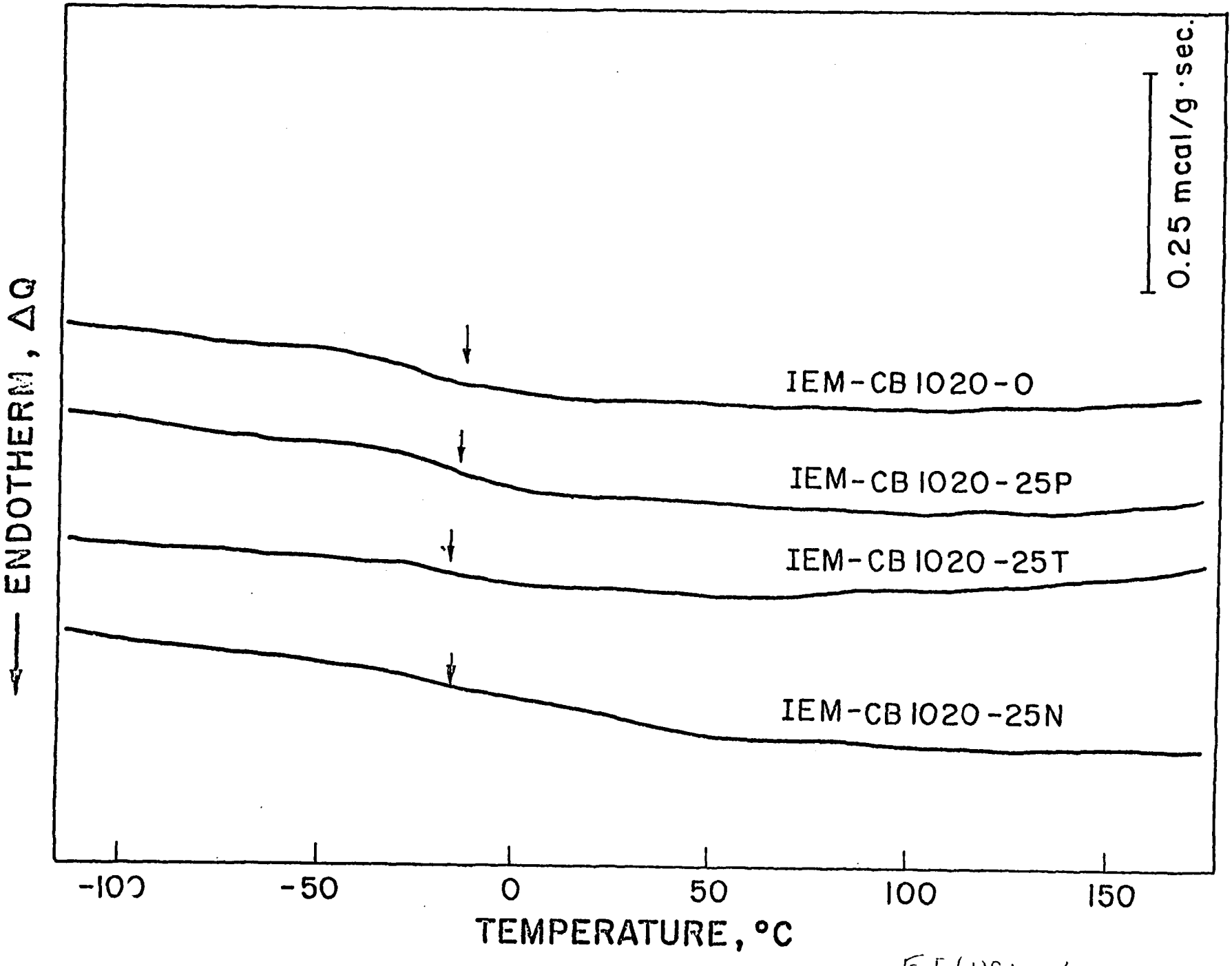
0.25 mcal/g·sec.
IEM-CB1020-0
IEM-CB1020-25P
IEM-CB1020-25T
IEM-CB1020-25N
← ENDOTHERM, ΔQ
-100
-50
0
50
100
150
TEMPERATURE, °C

FIGURE 4

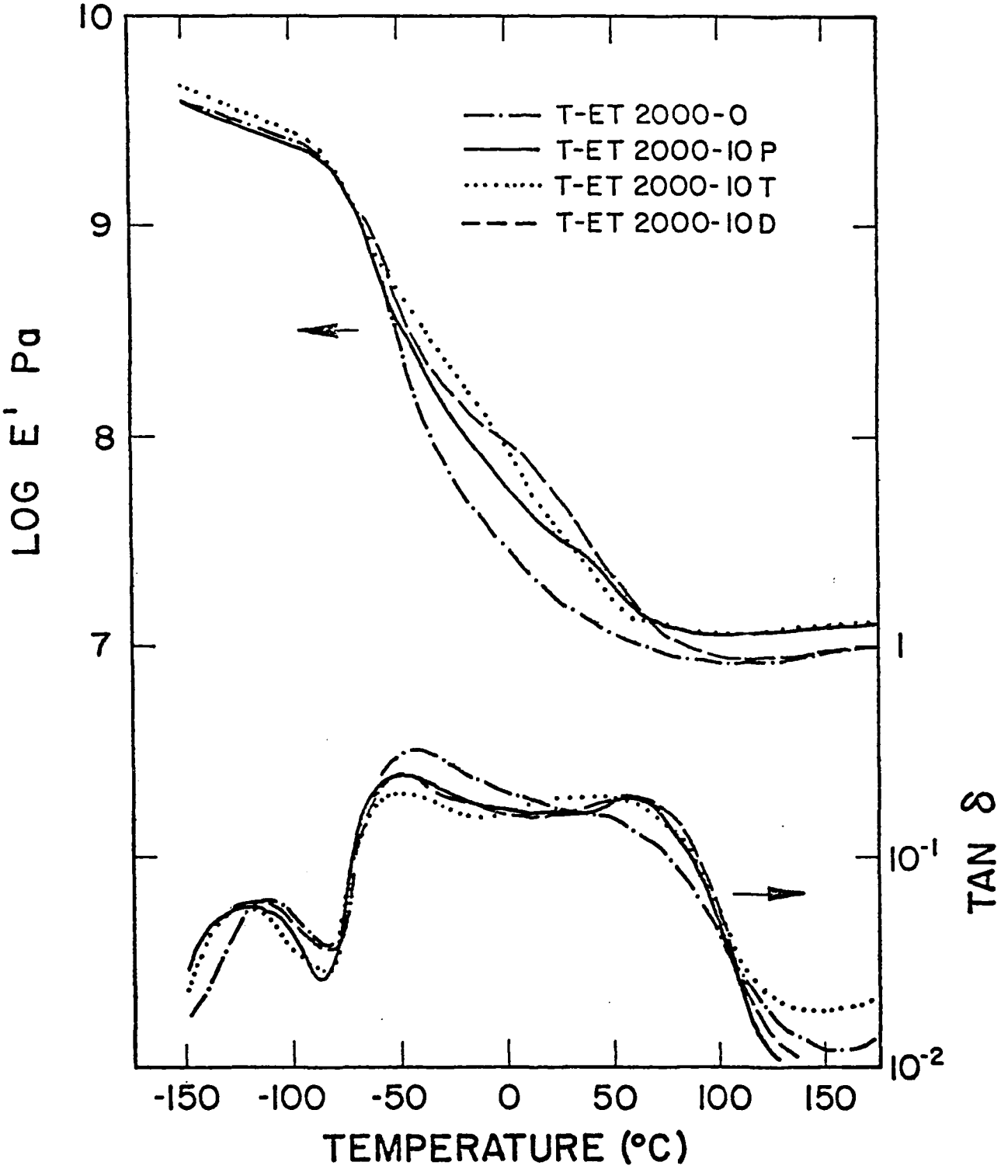
T-ET 2000-0
T-ET 2000-10 P
T-ET 2000-10 T
T-ET 2000-10 D
LOG E' Pa
10
9
8
7
1
$10^{-1}$
$10^{-2}$
TAN δ
-150
-100
-50
0
50
100
150
TEMPERATURE (°C)

FIGURE 5

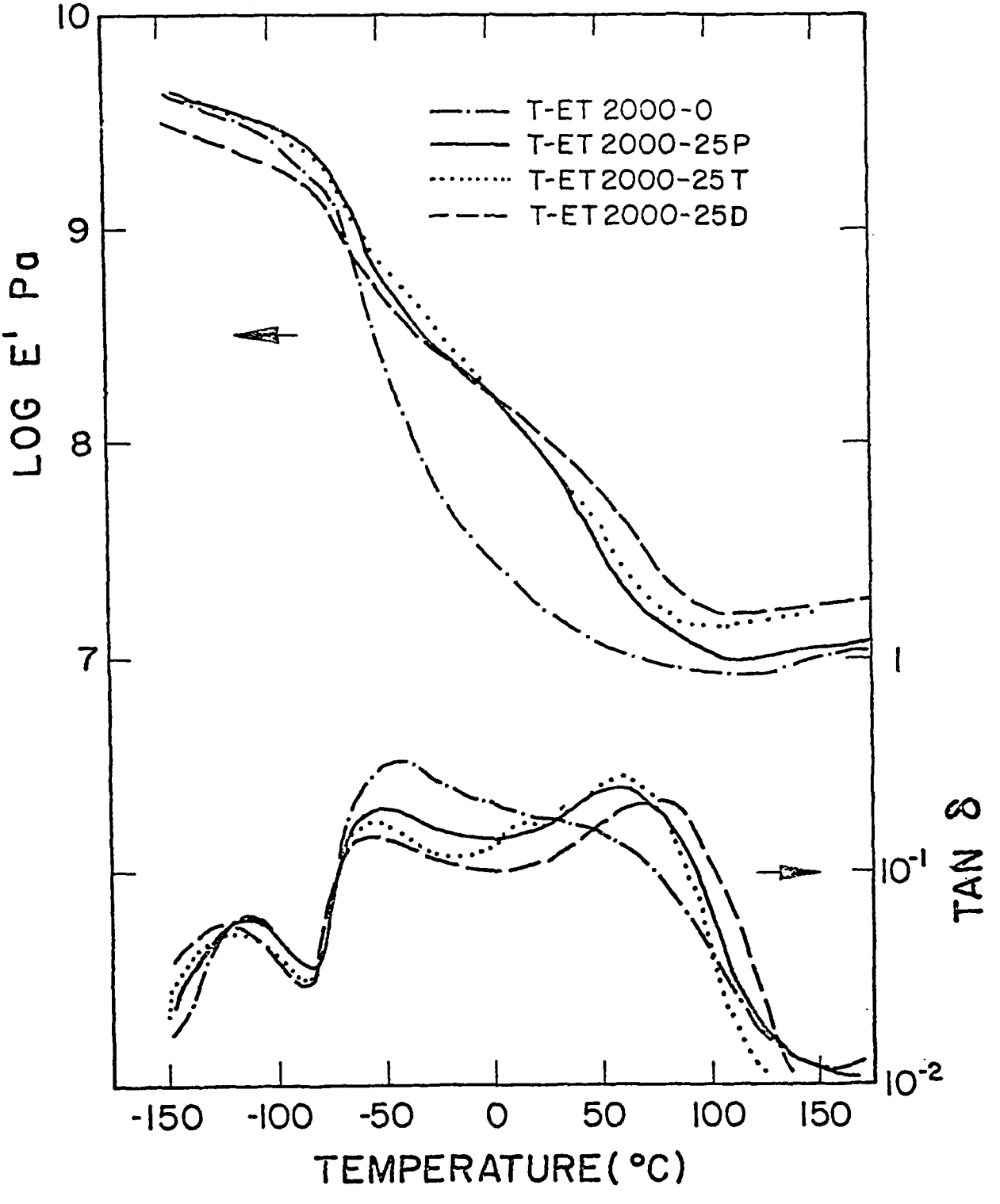
T-ET 2000-0
T-ET 2000-25P
T-ET 2000-25T
T-ET 2000-25D
LOG E' Pa
10
9
8
7
1
$10^{-1}$
$10^{-2}$
TAN δ
-150
-100
-50
0
50
100
150
TEMPERATURE(°C)

FIGURE 6

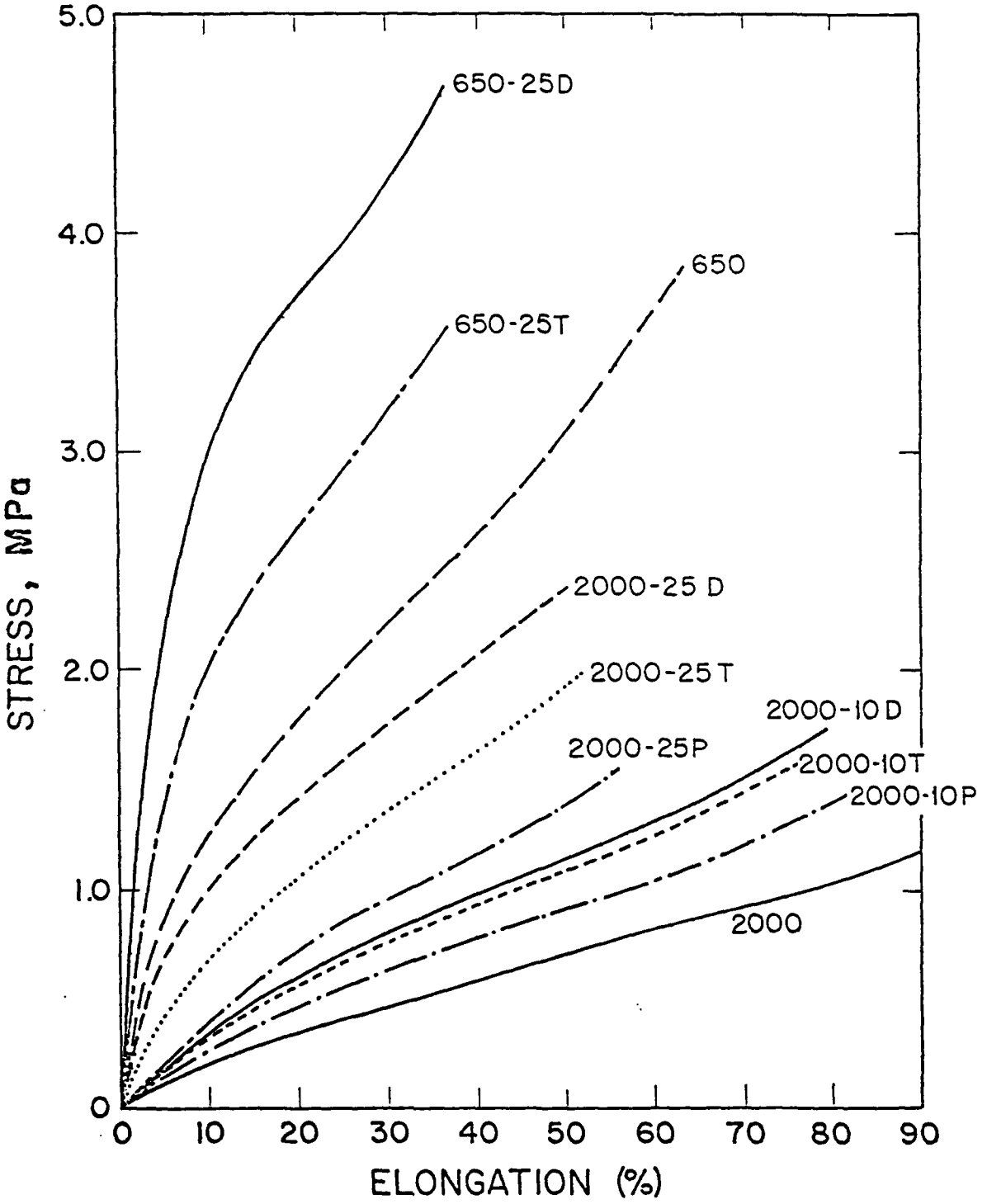
5.0
4.0
3.0
2.0
1.0
0
STRESS, MPa
650-25D
650
650-25T
2000-25 D
2000-25T
2000-10 D
2000-25P
2000-10T
2000-10P
2000
0
10
20
30
40
50
60
70
80
90
ELONGATION (%)

FIGURE 7

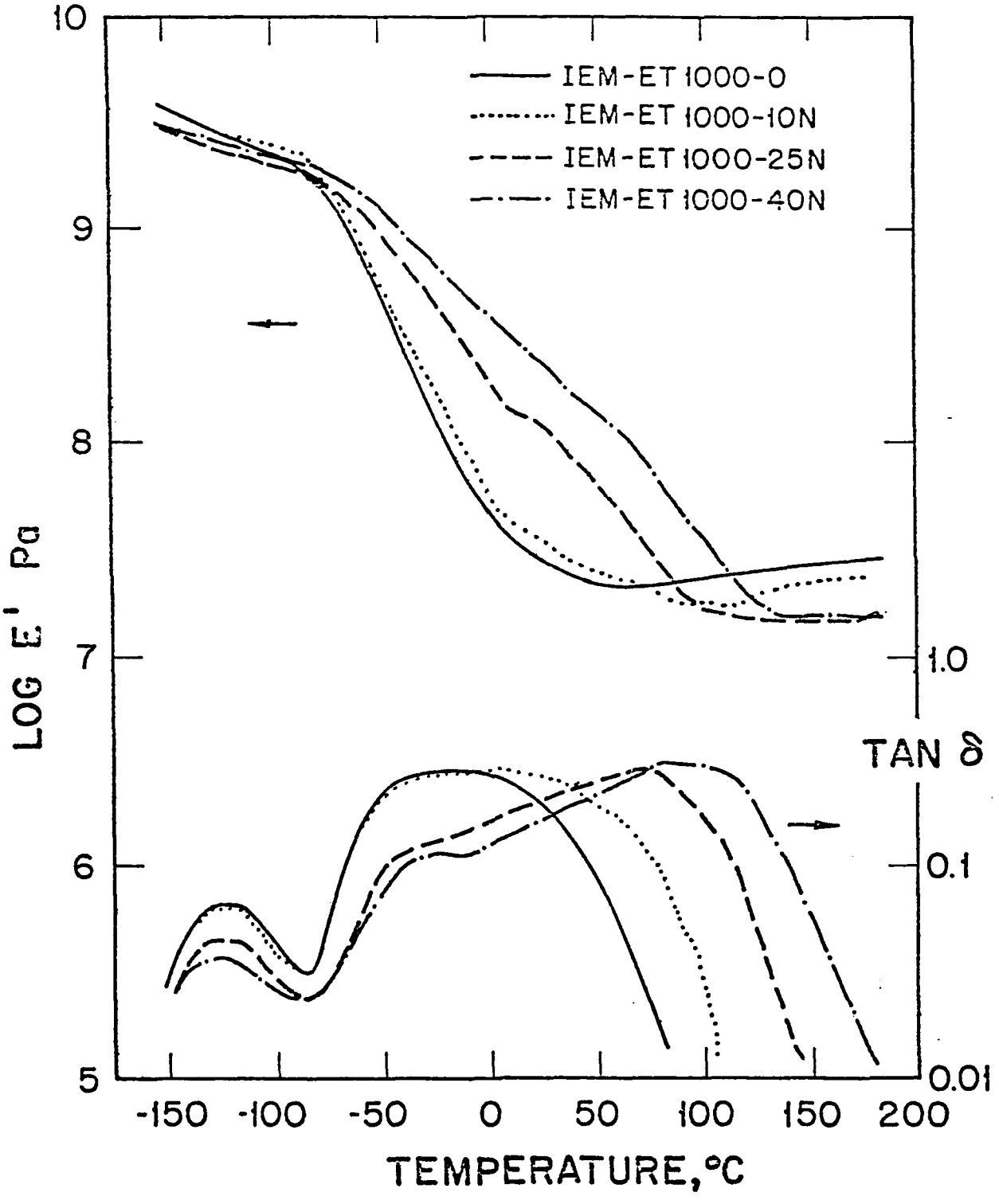
IEM-ET 1000-0
IEM-ET 1000-10N
IEM-ET 1000-25N
IEM-ET 1000-40N
LOG E' Pa
TAN δ
TEMPERATURE, °C
10
9
8
7
6
5
1.0
0.1
0.01
-150
-100
-50
0
50
100
150
200

FIGURE 8

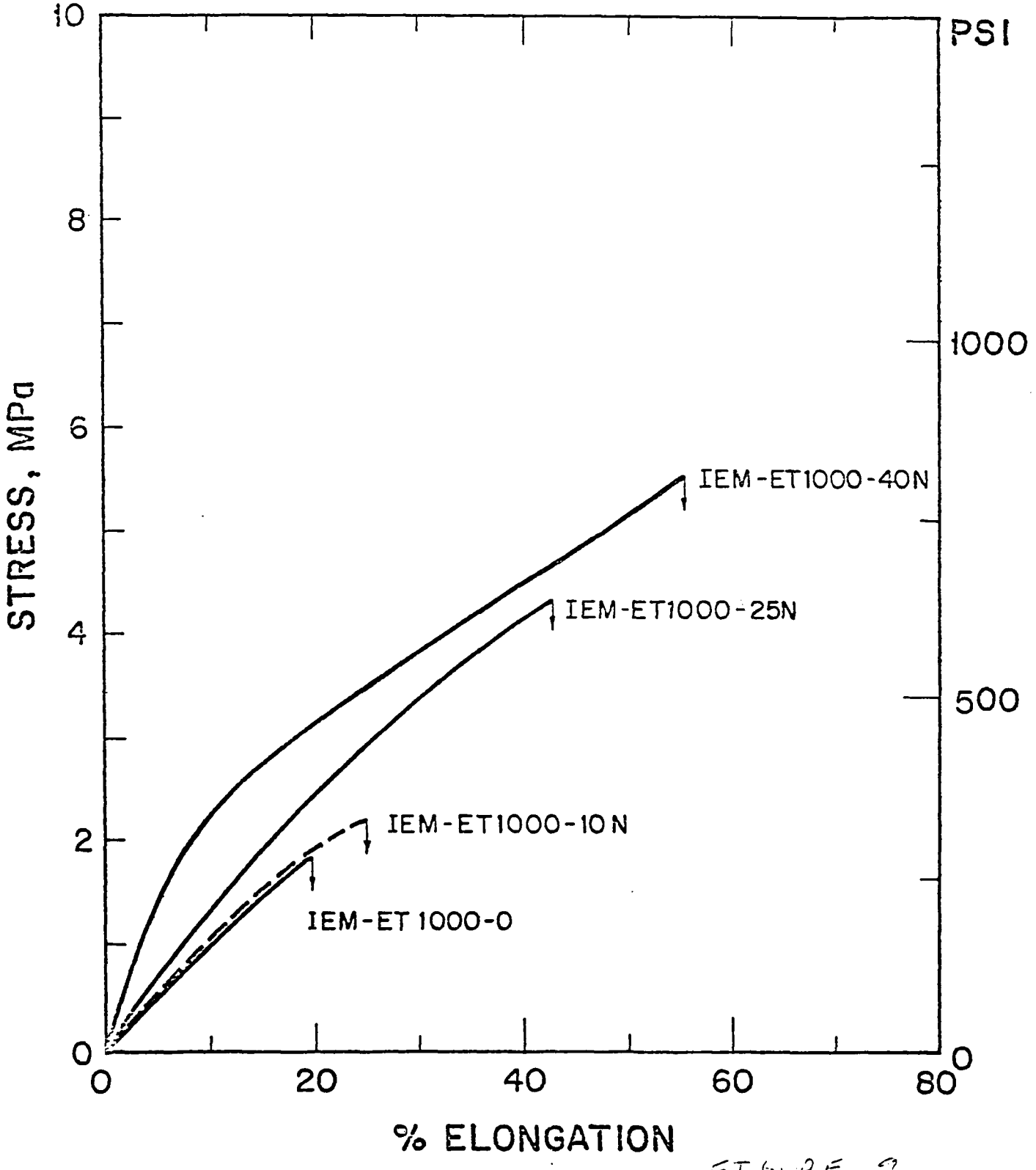
10
8
6
4
2
0
PSI
1000
500
0
STRESS, MPa
IEM-ET1000-40N
IEM-ET1000-25N
IEM-ET1000-10N
IEM-ET1000-0
0
20
40
60
80
% ELONGATION

FIGURE 9

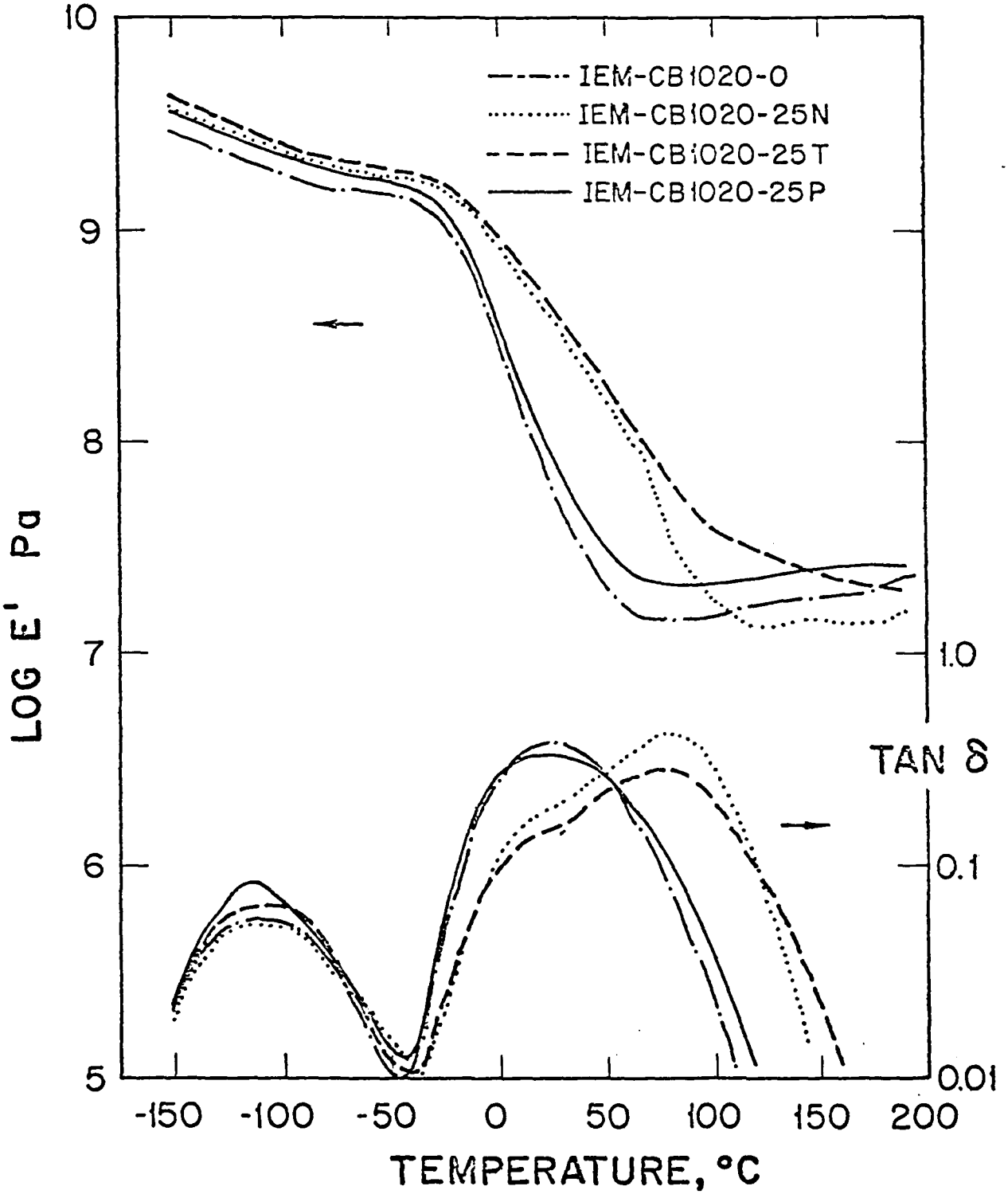
IEM-CB1020-0
IEM-CB1020-25N
IEM-CB1020-25T
IEM-CB1020-25P
LOG E' Pa
TAN δ
TEMPERATURE, °C
10
9
8
7
6
5
1.0
0.1
0.01
-150
-100
-50
0
50
100
150
200

FIGURE 10

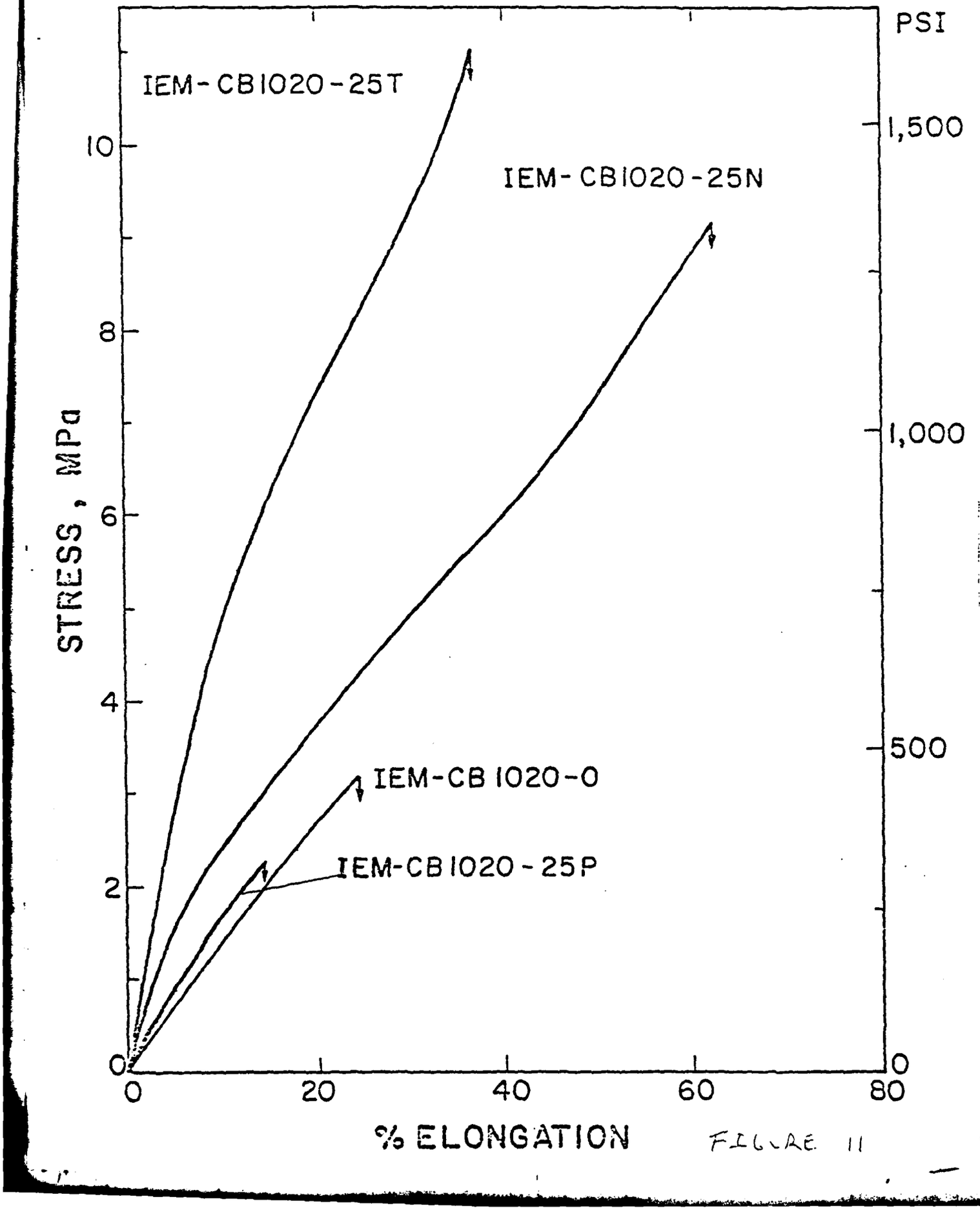
IEM-CB1020-25T
IEM-CB1020-25N
IEM-CB1020-0
IEM-CB1020-25P
STRESS, MPa
PSI
0
2
4
6
8
10
0
500
1,000
1,500
0
20
40
60
80
% ELONGATION

FIGURE 11

DL/413/83/01
GEN/413-2

# TECHNICAL REPORT DISTRIBUTION LIST, GEN

| | No. Copies |
|---|---|
| Office of Naval Research<br>Attn: Code 413<br>800 N. Quincy Street<br>Arlington, Virginia 22217 | 2 |
| ONR Pasadena Detachment<br>Attn: Dr. R. J. Marcus<br>1030 East Green Street<br>Pasadena, California 91106 | 1 |
| Commander, Naval Air Systems Command<br>Attn: Code 310C (H. Rosenwasser)<br>Washington, D.C. 20360 | 1 |
| Naval Civil Engineering Laboratory<br>Attn: Dr. R. W. Drisko<br>Port Hueneme, California 93401 | 1 |
| Superintendent<br>Chemistry Division, Code 6100<br>Naval Research Laboratory<br>Washington, D.C. 20375 | 1 |
| Defense Technical Information Center<br>Building 5, Cameron Station<br>Alexandria, Virginia 22314 | 12 |
| DTNSRDC<br>Attn: Dr. G. Bosmajian<br>Applied Chemistry Division<br>Annapolis, Maryland 21401 | 1 |
| Naval Ocean Systems Center<br>Attn: Dr. S. Yamamoto<br>Marine Sciences Division<br>San Diego, California 91232 | 1 |
| Naval Ocean Systems Center<br>Attn: Technical Library<br>San Diego, California 92152 | 1 |
| Naval Weapons Center<br>Attn: Dr. A. B. Amster<br>Chemistry Division<br>China Lake, California 93555 | 1 |
| Scientific Advisor<br>Commandant of the Marine Corps<br>Code RD-1<br>Washington, D.C. 20380 | 1 |
| Dean William Tolles<br>Naval Postgraduate School<br>Monterey, California 93940 | 1 |
| U.S. Army Research Office<br>Attn: CRD-AA-IP<br>P.O. Box 12211<br>Research Triangle Park, NC 27709 | 1 |
| Mr. Vincent Schaper<br>DTNSRDC Code 2830<br>Annapolis, Maryland 21402 | 1 |
| Mr. John Boyle<br>Materials Branch<br>Naval Ship Engineering Center<br>Philadelphia, Pennsylvania 19112 | 1 |
| Mr. A. M. Anzalone<br>Administrative Librarian<br>PLASTEC/ARRADCOM<br>Bldg 3401<br>Dover, New Jersey 07801 | 1 |

DL/413/83/01
356B/413-2

# TECHNICAL REPORT DISTRIBUTION LIST, 356B

Dr. C. L. Schilling
Union Carbide Corporation
Chemical and Plastics
Tarrytown Technical Center
Tarrytown, New York 10591

Dr. A. G. MacDiarmid
Department of Chemistry
University of Pennsylvania
Philadelphia, Pensylvania 19174

Dr. E. Fischer, Code 2853
Naval Ship Research and
Development Center
Annapolis, Maryland 21402

Dr. H. Allcock
Department of Chemistry
Pennsylvania State University
University Park, Pennsylvania 16802

Dr. M. Kenney
Department of Chemistry
Case Western University
Cleveland, Ohio 44106

Dr. R. Lenz
Department of Chemistry
University of Massachusetts
Amherst, Massachusetts 01002

Dr. M. David Curtis
Department of Chemistry
University of Michigan
Ann Arbor, Michigan 48105

NASA-Lewis Research Center
Attn: Dr. T. T. Serafini, MS 49-1
21000 Brookpark Road
Cleveland, Ohio 44135

Dr. J. Griffith
Naval Research Laboratory
Chemistry Section, Code 6120
Washington, D.C. 20375

Professor G. Wnek
Department of Materials Science
and Engineering
Massachusetts Institute of Technology
Cambridge, Massachusetts 02139

Dr. R. Soulen
Contract Research Department
Pennwalt Corporation
900 First Avenue
King of Prussia, Pennsylvania 19406

Dr. G. Goodman
Globe-Union Incorporated
5757 North Green Bay Avenue
Milwaukee, Wisconsin 53201

Dr. Martin H. Kaufman
Code 38506
Naval Weapons Center
China Lake, California 93555

Dr. C. Allen
Department of Chemistry
University of Vermont
Burlington, Vermont 05401

Professor R. Drago
Department of Chemistry
University of Florida
Gainesville, Florida 32611

Dr. D. L. Venezky
Code 6130
Naval Research Laboratory
Washington, D.C. 20375

Professor T. Katz
Department of Chemistry
Columbia University
New York, New York 10027

Professor James Chien
Department of Chemistry
University of Massachusetts
Amherst, Massachusetts 01002

Professor J. Salamone
Department of Chemistry
University of Lowell
Lowell, Massachusetts 01854

CAPT J. J. Auborn, USNR
AT&T Bell Laboratories
Room 6F-211
600 Mountain Avenue
Murray Hill, New Jersey 07974

DL/413/83/01
356B/413-2

# TECHNICAL REPORT DISTRIBUTION LIST, 356B

Professor D. Grubb
Department of Materials Science
and Engineering
Cornell University
Ithaca, New York 14853

Professor T. Marks
Department of Chemistry
Northwestern University
Evanston, Illinois 60201

Professor C. Chung
Department of Materials Engineering
Rensselaer Polytechnic Institute
Troy, New York 12181

Professor Malcolm B. Polk
Department of Chemistry
Atlanta University
Atlanta, Georgia 30314

Dr. D. B. Cotts
SRI International
333 Ravenswood Avenue
Menlo Park, California 94205

Dr. Kurt Baum
Fluorochem, Inc.
680 S. Ayon Avenue
Azuza, California 91702

Professor H. Hall
Department of Chemistry
University of Arizona
Tucson, Arizona 85721

Professor G. Whitesides
Department of Chemistry
Harvard University
Cambridge, Massachusetts 02138

Professor H. Ishida
Department of Macromolecular Science
Case Western University
Cleveland, Ohio 44106

Dr. K. Paciorek
Ultrasystems, Inc.
P.O. Box 19605
Irvine, California 92715

Professor D. Seyferth
Department of Chemistry
Massachusetts Institute of Technology
Cambridge, Massachusetts 02139

Dr. G. Bryan Street
IBM Research Laboratory, K32/281
San Jose, California 95193


ATE
LME